Iranian Journal of Hydrogen & Fuel Cell 1(2018) 1-11

Iranian Journal of Hydrogen & Fuel Cell

IJHFC

Journal homepage://ijhfc.irost.ir

Preparation of Ni-P-CeO_2 electrode and study on electrocatalytic properties for hydrogen evolution reaction

A.R. Madram[1,*] , M. Mohebbi[2], M. Nasiri[2], M.R. Sovizi[1]

[1] **Faculty of Chemistry and Chemical Engineering, Malek-Ashtar University of Technology, Tehran 15875-1774, IRAN.**
[2] **Department of Applied Chemistry, Malek-Ashtar University of Technology, Isfahan 83145-115, IRAN.**

Article Information

Article History:

Received:
02 Feb 2018
Received in revised form:
05 Jun 2018
Accepted:
07 Jun 2018

Keywords

Hydrogen evolution reaction (HER)
Ni-P-CeO_2
Electrocatalytic activity
Electrochemical impedance spectroscopy (EIS)

Abstract

In this study ternary Ni-P-CeO_2 catalysts were first synthesized by the Co-electrodeposition method on a copper substrate and then characterized by means of microstructural and electrochemical techniques toward a hydrogen evolution reaction (HER). Also, for comparison other catalysts such as Ni-CeO_2, Ni-P, and Ni were prepared and characterized by the same methods. The microstructure of the investigated catalysts was characterized by scanning electron microscopy (SEM) coupled with energy dispersive X-ray spectrometry (EDX) and X-ray diffraction (XRD) methods. The electrochemical efficiency of all investigated catalysts was studied based on electrochemical data obtained from electrochemical impedance spectroscopy (EIS) and steady-state polarization Tafel curves in 1 M NaOH solution. The results showed that microstructural properties play an essential role in the high electrocatalytic activity of Ni-P-CeO_2. Furthermore, it was observed that the HER mechanism for all investigated systems was Volmer-Heyrovsky with a Volmer step as the rate determining step (RDS). The Ni-P-CeO_2 catalyst, as the most active catalyst in this work, was characterized by an exchange current density of j_0=168.0 μAcm^{-2}, a Tafel slope of b=-162.0 $mV.dec^{-1}$, and overpotential at j=250 $mAcm^{-2}$; η_{250}=-143.0 mV.

1. Introduction

Fossil fuels as the main source of energy for today's world are one of the most important causes in the evolution of the green-house gas, CO_2. Hydrogen is a promising replacement candidate for fossil fuels because of its outstanding specifications such as being abundant, regenerable and a clean source

*Corresponding Author's Fax: +982122962257
E-mail address: ar.madram@gmail.com

doi:10.22104/ijhfc.2018.2758.1167

of energy. Water electrolysis is the only method for direct production of very high purity hydrogen gas [1]. However, water electrolysis is currently limited by its high electricity consumption. From an electrochemical point of view, for the decrease of the hydrogen cost it should be decrease the HER overpotential [2]. Although Pt is the best candidate with the highest electrocatalytic activity and lowest overpotential toward the HER, its scarcity and high cost restrict its wide usage in the production of hydrogen [1, 2]. Also, Pt is not stable in a chloride solution for long term performance, for example in chlor-alkali industries. Therefore, numerous studies have been performed to find alternative non-precious metals, catalysts or composites with high electrocatalytic activity and stability toward the HER [3-12]. As the most studied catalytic material, Ni and its alloys with other metals or non-metals have been prepared and studied by various methods to increase its surface area or intrinsic activity (synergetic effect) for the HER [13-15]. Ni-P material has been found to be one of the most interesting catalysts with high stability and good electrocatalytic activity for the HER in alkaline solution [16, 17]. Moreover, various studies were performed to increase its activity toward the HER by increasing its intrinsic activity or real surface area. On the other hand, rare earth (RE) elements are also very interesting materials because of their many unique properties. They are used for various applications such as corrosion resistance, electrocatalytic activity and superconductivity. Additionally, some RE-based catalysts have been studied for the HER, especially in alkaline solutions [1, 18, 19]. However, the literature on RE-based catalysts applications for the HER is scarce, and there are few works about their kinetic parameters and electrocatalytic activities.

In the present work the interesting properties of CeO_2 and Ni-P were integrated and a Ni-P-CeO_2 catalyst was prepared by Co-electrodeposition methods as a new cathode material for the HER. Then, the electrochemical activity and mechanism of the HER on the investigated catalyst was studied by polarization Tafel curves and electrochemical impedance spectroscopy (EIS). Additionally, the stability of the Ni-P-CeO_2 catalyst for the HER in alkaline solution was studied at high current densities. All electrochemical studies were performed in 1M NaOH.

2. Experimental

Copper rod was used as the substrate. Before the electrodeposition process, the sides of the copper substrate were sealed in a heat-shrinkable plastic tube. Its apparent surface area for the electrodeposition was 0.196 cm^2. Substrates were then polished by 600 grade SiC paper (3µm diamond grain) and immerse for 2 min in 20 wt.% NaOH at 77 °C. After that they were washed with 10 wt.% HCl and then again with double distilled water. Finally, the substrates were degreased with acetone and then washed with doubly distilled water before use. A three-electrode cell that consisted of: 1. a Pt plate as a counter electrode (anode), 2. commercial Ag-AgCl with 3 M KCl as a reference electrode, and 3. copper substrate was used as a working electrode (cathode). Electrodeposition of Ni, Ni-P, Ni-CeO_2 and Ni-P-CeO_2 were performed on copper substrate in the plating bath A, B, C and D, respectively, (Table 1) under constant current. The deposition was based on a modulated pulse signal in the microsecond range. During the relatively long pulse of negative current the metal was deposited on the substrate. All chemicals used were of analytical grade.

3. Measurements

The morphology of the surface of the catalysts was determined by scanning electron microscopy (SEM). The instrument used was a VEGA3 XMU, working at a 20 kV and equipped with the SEM software. The catalyst composition and crystalline structure were analysedby quantitative energy dispersive

Table 1.Composition and deposition conditions.

Composition and conditions	Bath			
	A (Ni)	B (Ni-P)	C (Ni-CeO_2)	D (Ni-P-CeO_2)
$NiSO_4$. $7H_2O$ (g/l)	320.0	320.0	320.0	320.0
NiC_{l2}.$6H_2O$ (g/l)	60.0	60.0	60.0	60.0
H_3BO_3 (g/l)	40.0	40.0	40.0	40.0
NaH_2PO_2 (g/l)	0.0	100.0	0.0	100.0
$C_6H_8O_7$. H_2O (g/l) (citric acid)	0.0	0.0	10.0	10.0
CeO_2 (g/l)	0.0	0.0	15.0	15.0
pH	4.3			
Time (min)	30.0			
Magnetic stirring speed (rpm)	220			
Applied current density (mA/cm^{-2})	23.0			
Temperature (°C)	47.0			

spectroscopy (EDX, VEGA3 XMU) coupled with SEM and X ray diffraction (XRD) analysis (Philips-X'Pert-MPD) using Cu Kα wavelength of 1.5418 Å from 20° to 80° at a speed of 5° min^{-1}.

All the electrochemical tests for the HER studies were performed in 1 M NaOH solution at room temperature. A thermostated water bath was used as a temperature controller. An Hg/HgO/OH- electrode and a Pt foil (5 cm^2) was used as the reference and counter electrode, respectively.

Steady-state polarization Tafel curves and the EIS measurements were used to investigate the electrocatalytic activities of the catalysts. In order to obtain the stationary conditions necessary for polarization Tafel curves and EIS studies, the working electrodes were polarized at 100 mA for 5 h in 1 M NaOH at 298 K. Kinetic parameters, such as overpotential at the current density of 250 mA cm^{-2} (η_{250}), exchange current density (j_o) and Tafel slope (b), were evaluated for all investigated catalysts.

The EIS measurements were performed in a wide range of frequency, 10 kHz to 100 mHz, and the ac amplitude was 10 mV. Measurements were carried out by using a Potentiostat/Galvanostat Biologic Sp-150. The EIS data were estimated using ZView® software and the complex nonlinear least-square (CNLS) method [9].

4. Results and discussion

4.1. Surface morphology and structure

Surface morphology of the investigated electrode was carried out by the SEM technique. The micrographs of the Ni (a), Ni-P (b), Ni-CeO_2 (c) and Ni-P-CeO_2 (d) catalysts are shown in Fig. 1. As can see in these images, there are significant differences in the morphology of the investigated electrodes, particularly for the Ni CeO_2 and Ni P CeO_2 catalyst. Fig. 1(d) presents a micro-roughness and cauliflower like image for Ni P CeO_2. Obviously, the porosity of this composite catalyst is higher than the other investigated catalysts and probably predicts its high electrocatalytic activity toward the HER. The uniformity and distribution of the constituent elements of Ni P CeO_2, evaluated by the SEM mapping, also are shown in Fig. 1 (e, f, g and h for Ni, P, Ce and O, respectively). The contents of Ni, P and Ce in the investigated catalysts were evaluated by the EDX technique and the results are presented in Table 2. A typical EDX spectrum obtained from the surface of the Ni P CeO_2 electrode is presented in Fig. 2. These results revealed that the content of Ni, P, Ce and O are of 71.0 wt. %, 8.6 wt. %, 6.9 wt. % and 13.5 wt. %, respectively.

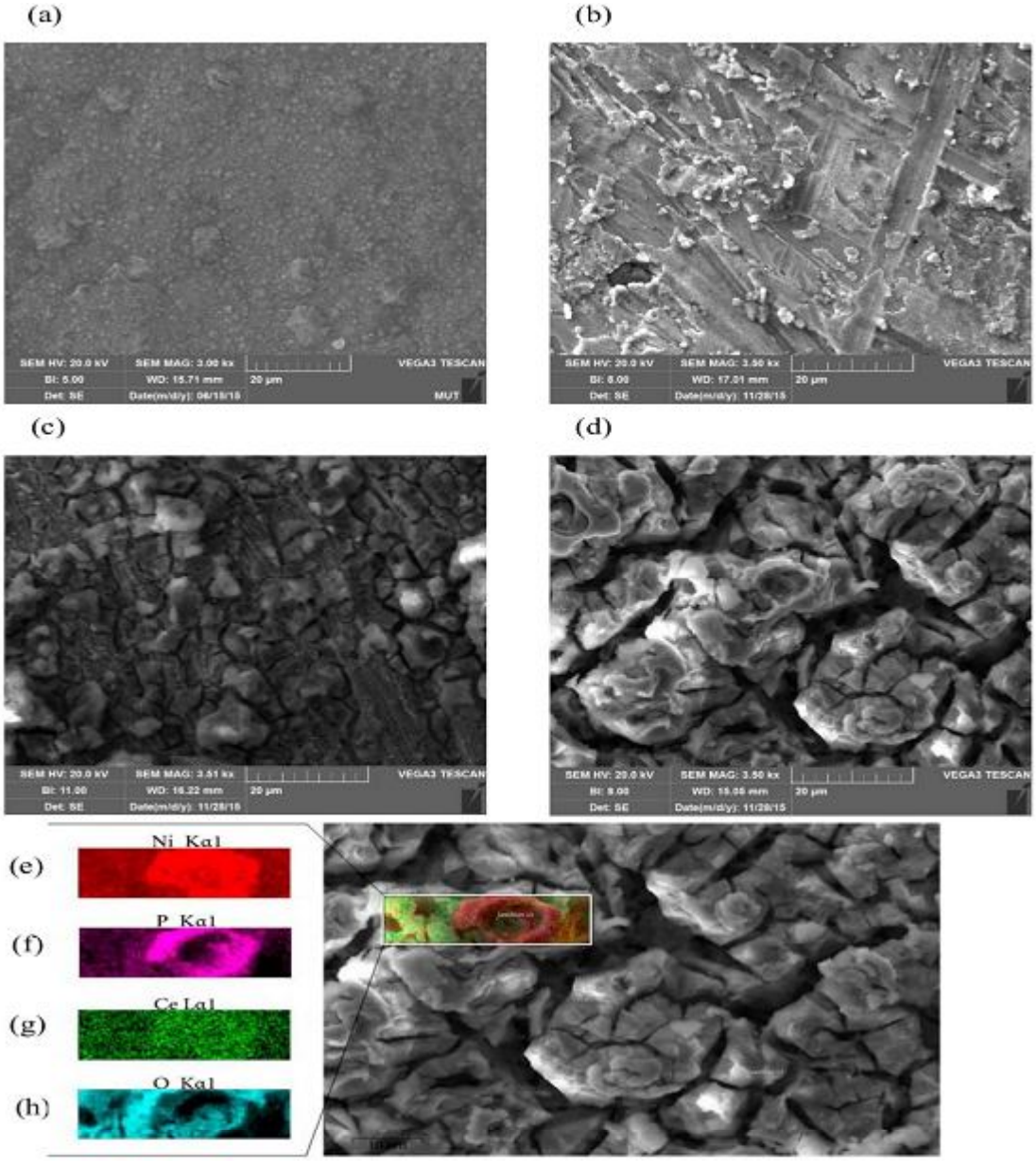

Fig. 1. Scanning electron micrographs of the (a) Ni, (b) Ni-P, (c) Ni- CeO_2 and (d) Ni P CeO_2. Red image of the (e) nickel, pink image of the (f) phosphor, green image of the (g) cerium and blue image of the (h) oxygen displayed in the element mapping

Table 2. Composition of Ni, Ni-P, Ni-CeO_2 and Ni-P-CeO_2 Electrodes.

Deposition	Ni, wt%	Ce, wt%	P, wt%	O, wt%
Ni	100.0	0.0	0.0	0.0
Ni-P	84.0	0.0	12.1	3.9
Ni-CeO_2	74.7	5.8	0.0	19.5
Ni-P-CeO_2	71.0	6.9	8.6	13.5

Steady-state polarization Tafel curves and the EIS measurements were used to investigate the electrocatalytic activities of the catalysts. In order to obtain the stationary conditions necessary for polarization Tafel curves and EIS studies, the working electrodes were polarized at 100 mA for 5 h in 1 M NaOH at 298 K. Kinetic parameters, such as overpotential at the current density of 250 mA cm^{-2} (η_{250}), exchange current density (j_o) and Tafel slope (b), were evaluated for all investigated catalysts.

The EIS measurements were performed in a wide range of frequency, 10 kHz to 100 mHz, and the ac amplitude was 10 mV. Measurements were carried out by using a Potentiostat/Galvanostat Biologic Sp-150. The EIS data were estimated using ZView® software and the complex nonlinear least-square (CNLS) method [9].

4. Results and discussion

4.1. Surface morphology and structure

Surface morphology of the investigated electrode was carried out by the SEM technique. The micrographs of the Ni (a), Ni-P (b), Ni-CeO_2 (c) and Ni-P-CeO_2 (d) catalysts are shown in Fig. 1. As can see in these images, there are significant differences in the morphology of the investigated electrodes, particularly for the Ni CeO_2 and Ni P CeO_2 catalyst. Fig. 1(d) presents a micro-roughness and cauliflower like image for Ni P CeO_2. Obviously, the porosity of this composite catalyst is higher than the other investigated catalysts and probably predicts its high electrocatalytic activity toward the HER. The uniformity and distribution of the constituent elements of Ni P CeO_2, evaluated by the SEM mapping, also are shown in Fig. 1 (e, f, g and h for Ni, P, Ce and O, respectively). The contents of Ni, P and Ce in the investigated catalysts were evaluated by the EDX technique and the results are presented in Table 2. A typical EDX spectrum obtained from the surface of the Ni P CeO_2 electrode is presented in Fig. 2. These results revealed that the content of Ni, P, Ce and O are of 71.0 wt. %, 8.6 wt. %, 6.9 wt. % and 13.5 wt. %, respectively.

The crystal structure information of Ni-P-CeO_2 catalyst was examined by XRD analysis as shown in Fig. 3. The Ni P CeO_2 analysis of XRD indicated that Ni P CeO_2 is amorphous in structure and exhibited a single broad peak.

4.2. Polarization Tafel curve

The HER electrocatalytic performance of the investigated catalysts in 1 M NaOH are shown in Fig. 4. Obviously, one slope for all Tafel curves can be seen and this predicted the same mechanism of the HER on the surface of all investigated materials. The parameters, such as b, η_{250} and jo, can be calculated from the classical Tafel equation [20].

$$\eta_c = a + b\log j$$

$$a = -\frac{2.3RT}{\alpha nF}\log j_o \text{ and } b = \frac{2.3RT}{\alpha nF}$$

Where, η_c (V) is the cathodic over potential, j (A) is the current density, (a) and (b) are the intercept and Tafel slope, respectively. Other parameters are defined as: transfer coefficient (α), gas constant (R), absolute temperature (T), Faraday constant (F) and number of electrons exchanged (n) [20]. The kinetic parameters, b, j_o, α and η_{250} were estimated from the linear part of the Tafel curves (Fig. 4) and are presented in Table 3. The highest value of jo (168.0 μA cm^{-2}) and lowest value of η_{250} (-143.0 mV) were observed for the Ni-P-CeO_2 catalyst. It was interesting that the value of η_{250} for Ni P CeO_2 was significantly smaller than Ni CeO_2 (-323.0 mV) and Ni P (-413.0 mV). In addition, the Tafel slope and charge-transfer coefficient α (b =2.3RT⁄αnF) was used to find out the rate-determining step (RDS) and HER mechanism [21]. The HER in an alkaline solution is a multi-step reactions. The Volmer reaction is an electrochemical adsorption step. The Heyrovsky reaction is an electrochemical desorption step and the Tafel reaction is a chemical desorption [22, 23]. As reported previously [20], when the

b parameter is around 120 mVdec^{-1}, the proton discharge electrosorption step (Volmer reaction) is RDS in the HER mechanism. Also, if the Heyrovsky or Tafel reaction is RDS, the values of b should be around 40 or 30 mV dec^{-1}, respectively. It can see in Table 3 that the values of the b parameters for Ni-CeO_2 and Ni-P-CeO_2 catalysts are 151.0 to 162.0 mV dec^{-1} respectively. The obtained values for b were in good agreement with other previously reported Ni RE catalysts [18]. The results of this study indicated the RDS for all electrodes is the Volmer step. However, the measured Tafel slopes for all investigated electrode slightly deviated from the theoretical values, which can be explained by the formation of a thin surface oxide layer on the substrate [18, 24]. Also, the observed linearity in the Tafel curves at higher overpotentials for all investigated catalysts (Fig. 4) indicate that the HER mechanism

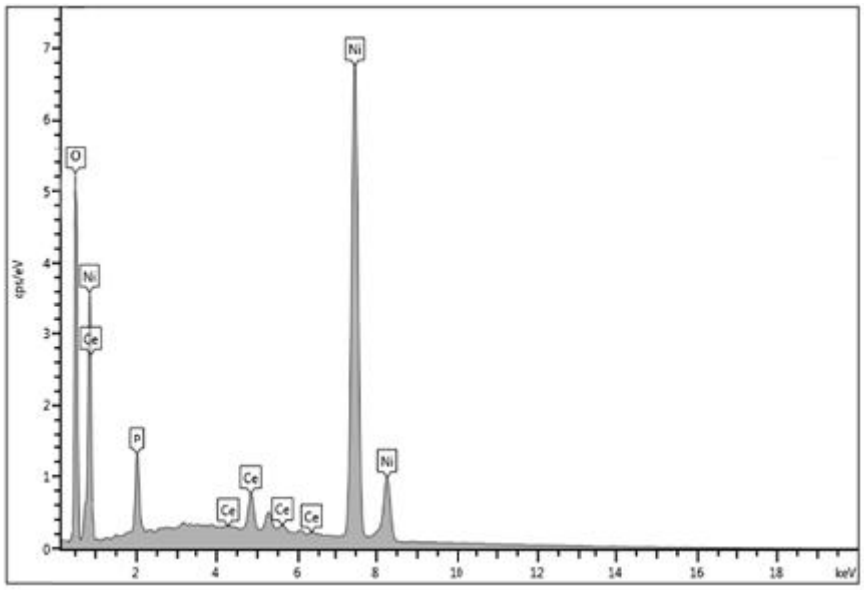

Fig. 2 EDX pattern of the Ni-P-CeO_2 electrode

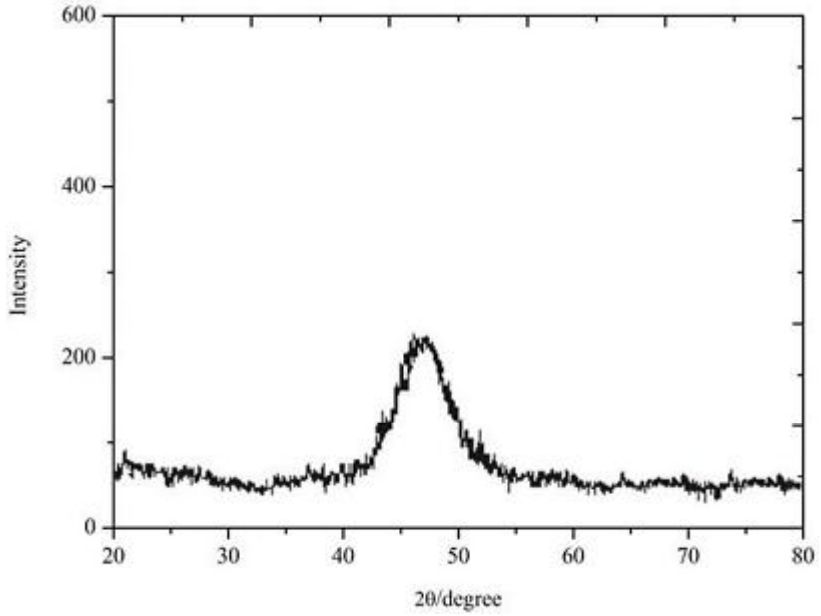

Fig. 3. XRD spectra of electrodeposited Ni-P-CeO_2 electrode

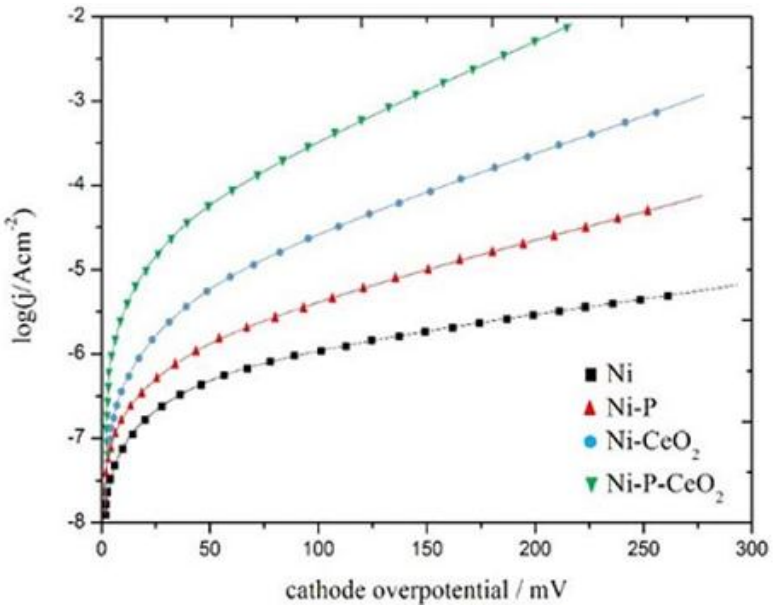

Fig. 4. Steady-state polarization Tafel curves on the investigated alloys for the HER in 1 M NaOH at 25 °C

is Volmer-Heyrovsky. Therefore, in the Tafel studies the Ni P CeO_2, as the most active catalyst in this study, is characterized by a Tafel slope of b=162.0 mV dec^{-1}, an exchange current density of j_o=168.0 μA cm^{-2}, an overpotential at current density 250 mA cm^{-2}: η_{250}=-143.0 mV, and a transfer coefficient of α=0.36. Also, the HER mechanism on its surface is Volmer Heyrovsky with a Volmer reaction as the RDS.

4.3. EIS measurements

The electrocatalytic performance of the Ni-P-CeO_2 catalyst as the highest active electrode towards the HER was studied using the EIS technique in 1 M NaOH at room temperature. Comparative investigations were performed on Ni, Ni-P and Ni CeO_2 catalysts under the same experimental conditions.

Nyquist plots for the Ni-P-CeO_2 catalyst and other electrodes at an overpotential of -200 mV are shown in Fig. 5. In general, two semicircles were obtained for the investigated catalysts over the explored frequency ranges. In order to analyze the results, the measured data were modelled using nonlinear least-square fitting analysis. The electrical circuit model is shown in Fig. 6. In this model, Rs is the solution resistance, Rct is the charge transfer resistance, CPE1 is a constant phase element related to the double-layer capacity of the surface (Cdl), CPE2 is the constant phase element of the pseudo-capacitance, and Rp simulate the frequency and potential dependto the adsorption process [8]. The CPE element was used due to the surface roughness or impurities (geometric factors).

The measurement data from the analysis of impedance spectra are reported in Table 4. The values of R_{ct} for Ni, Ni P, Ni CeO_2 and Ni P CeO_2 catalysts ranged from 22.51 to 0.76 Ω cm^2. Indeed, R_{ct} decreased significantly (~18 times) from Ni P to Ni P CeO_2 which may be due to the CeO_2 embedded into Ni P matrix. The real surface area was determined by comparison of C_{dl} for the investigated catalysts (Table 4) with 20 μFcm^{-2} for smooth nickel. The highest values of R_f were observed for Ni CeO_2 (2050.0) and Ni P CeO_2 (3900.0), which is in good agreement with the SEM observations. However, the high values of R_f for these catalysts can be a source for their electrocatalytic activity toward the HER.

Furthermore, dependence of R_{ct}^{-1} to overpotential was studied for the investigated catalysts and results are shown in Fig. 7. The slope of the R_{ct}^{-1}–η curves of all investigated catalysts ranged from 111 to 158 mV dec^{-1}, which are in good agreement with the polarization studies (Table 3 and Fig. 4) and predict

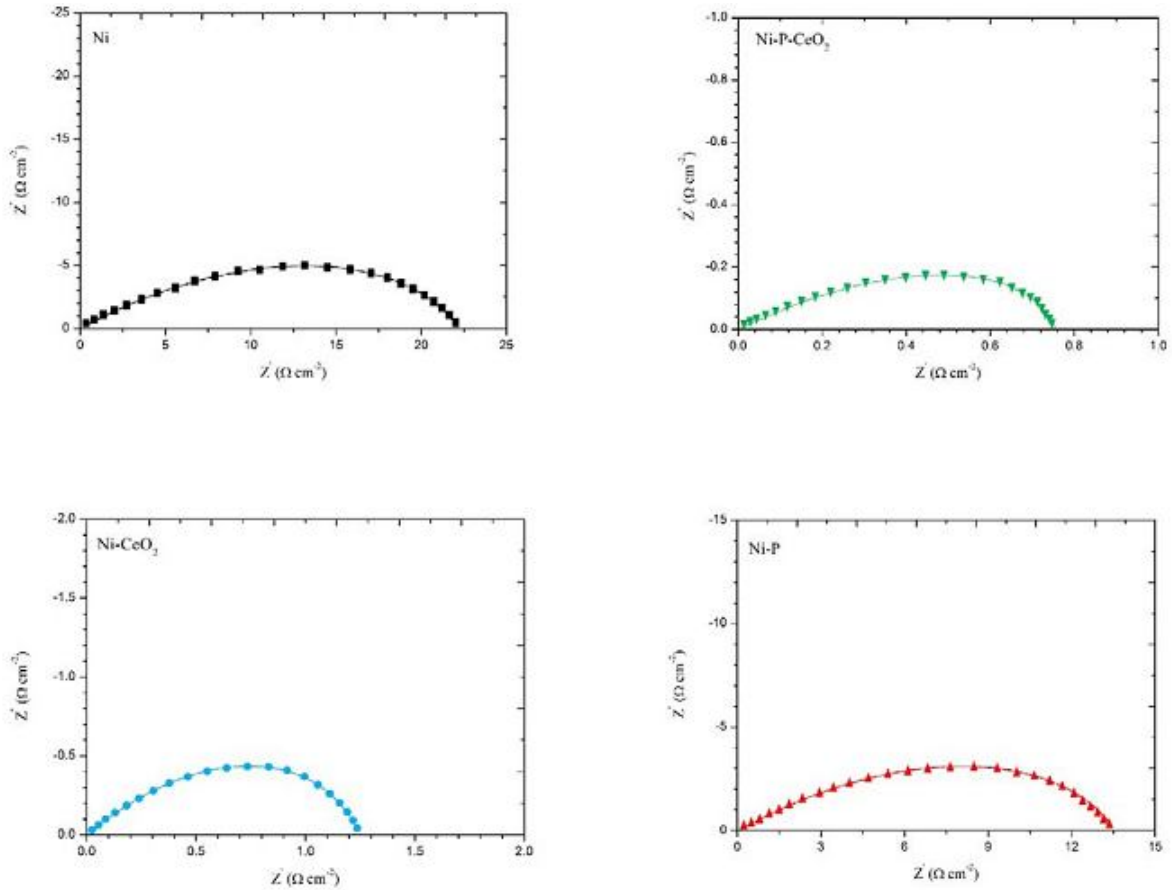

Fig. 5. Complex-plane plots of the HER on investigated catalysts at η=-200 mV in 1 M NaOH solution

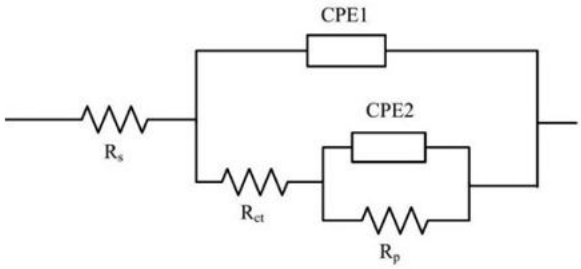

Fig. 6. Equivalent circuit used for fitting the ac impedance result

that the HER was performed via Volmer-Heyrovsky mechanism on all investigated systems.

4.5. Stability of Ni-P-CeO_2

In order to verify electrochemical and physical stability of the Ni P CeO_2 catalyst as the most active catalyst in this study, a galvanostatic test at a high current density (300 mA/cm^{-2}, i.e. the density usual used in industrial operations) was performed. Thus, the electrode was studied through long term (600 h) working experiments by operating at a constant applied current density, j=300 mA/cm^{-2} in 1 M NaOH and its potential response (chronoapotentiogram) was recorded (Fig. 8). This behavior showed that the response of the Ni P CeO_2 electrode is physically, chemically, and electrochemically stable for a relatively long-time for the HER in alkaline solutions.

Table 3. Electrocatalysis parameters of the HER obtained from the polarization curve recorded in 1 M NaOH solution at 25 °C.

Electrode	b/mV dec^{-1}	Jo/μA cm^{-2}	$-\eta_{250}$/mV	α
Ni	110.0±0.5	1.7±0.4	492.0±2.4	0.54
Ni-P	114.0±0.6	9.2±1.4	413.0±2.1	0.52
Ni-CeO2	151.0±1.5	90.2±1.1	323.0±2.3	0.39
Ni-P- CeO2	162.0±1.3	168.0± 1.2	143.0±1.7	0.36

Table 4. Values obtained for the investigated electrodes in 1 M NaOH by approximation of the EIS experimental data.

Electrode	$R_{ct}/\Omega\ cm^2$	C_{dl} (mF cm^{-2})	R_f
Ni	22.51±0.07	1.92±0.05	96.0
Ni-P	13.48±0.06	13.40±0.21	670.0
Ni- CeO_2	1.49±0.42	41.00±0.42	2050.0
Ni-P- CeO_2	0.76±0.32	78.00±0.64	3900.0

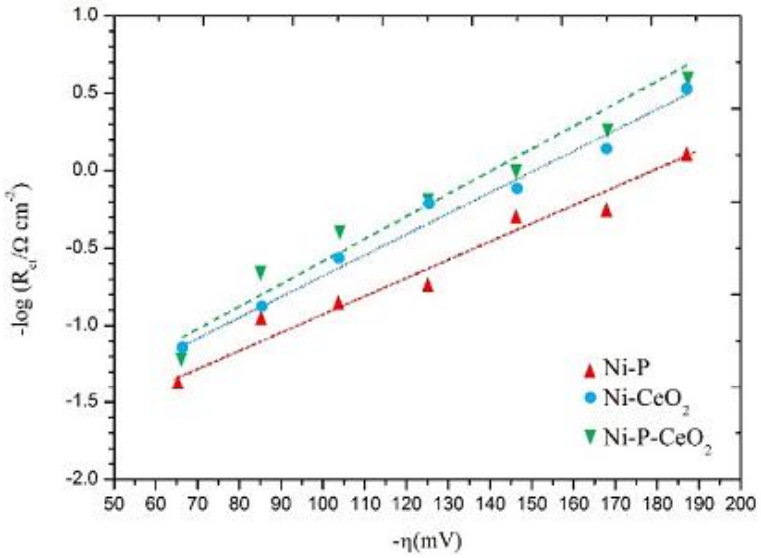

Fig. 7. –Log R_{ct}^{-1} against -η relationship for Ni-P, Ni-CeO_2 and Ni-P-CeO_2 alloys in 1 M NaOH solution at room temperature

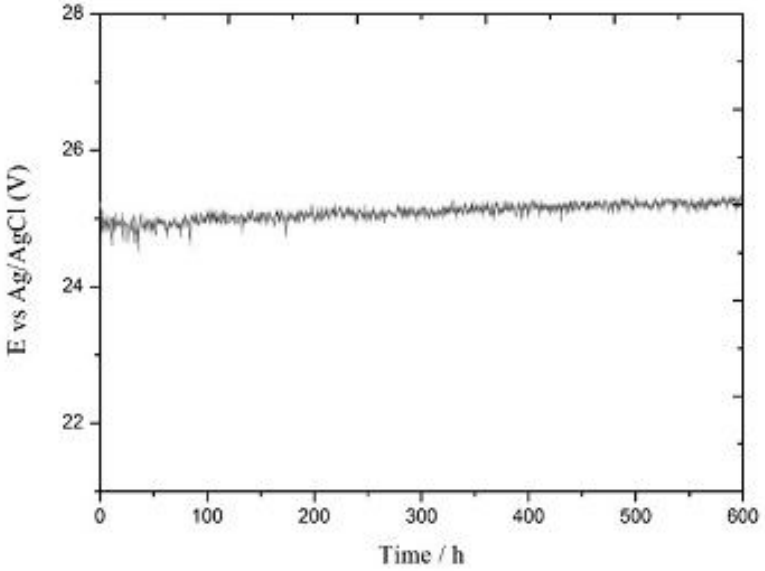

Fig. 8. Cathodic potential in HER for Ni-P-CeO_2 electrode (jo=300 mA/cm^{-2} in 1 M NaOH solution at 25 °C

5. Conclusions

The Ni-P-CeO_2 catalyst, as a new active catalyst toward HER, was prepared by Co-electrodeposition from a watts bath with CeO_2 particles. The morphology of the substrate surface and composition of the electrocatalyst was determined. Steady-state polarization and impedance measurements in 1 M NaOH solution at 25 °C were used to determine the electrocatalytic efficiency for the hydrogen evolution reaction. The results showed that the HER on Ni-P-CeO_2 was performed via the Volmer–Heyrovsky mechanism and a Volmer step as RDS. It was found that the electrocatalytic properties and stability toward the HER in alkaline solution at high current densities improved by incorporating CeO_2 in the Ni-P matrix. The Ni-P-CeO_2 catalyst is characterized by b=162.0 mV/dec^{-1}, η_{250}=-143.0 mV and j_o=168.0 μA cm^{-2}. Therefore, the results revealed that Ni-P-CeO_2 catalysts have good electrocatalytic activity compared to Ni-CeO_2.

References

[1] Cardoso DSP, Amaral L, Santos DMF, Šljukić B, Sequeira CAC, Macciò D, et al. "Enhancement of hydrogen evolution in alkaline water electrolysis by using nickel-rare earth alloys". International Journal of Hydrogen Energy. 2015, 40:4295.

[2] Cardoso JASB, Amaral L, Metin Ö, Cardoso DSP, Sevim M, Sener T, et al. "Reduced graphene oxide assembled Pd-based nanoalloys for hydrogen evolution reaction". International Journal of Hydrogen Energy. 2017, 42:3916.

[3] Chen Y-q, Zhang J-f, Wan L, Hu W-b, Liu L, Zhong C, et al. "Effect of nickel phosphide nanoparticles crystallization on hydrogen evolution reaction catalytic performance". Transactions of Nonferrous Metals Society of China. 2017, 27:369.

[4] He P, Yi X, Ma Y, Wang W, Dong F, Du L, et al. "Effect of Gd_2O_3 on the hydrogen evolution property of nickel–cobalt coatings electrodeposited on titanium substrate". Journal of Physics and Chemistry of Solids. 2011, 72:1261.

[5] Marceta Kaninski MP, Nikolic VM, Tasic GS, Rakocevic ZL. "Electrocatalytic activation of Ni electrode for hydrogen production by electrodeposition of Co and V species". International Journal of Hydrogen Energy. 2009, 34:703.

[6] Marini S, Salvi P, Nelli P, Pesenti R, Villa M, Kiros Y. "Stable and inexpensive electrodes for the hydrogen evolution reaction". International Journal of Hydrogen Energy. 2013, 38:11484.

[7] Rosalbino F, Delsante S, Borzone G, Angelini E. "Electrocatalytic behaviour of Co–Ni–R (R = Rare earth metal) crystalline alloys as electrode materials for hydrogen evolution reaction in alkaline medium". International Journal of Hydrogen Energy. 2008, 33:6696.

[8] Rosalbino F, Macciò D, Angelini E, Saccone A, Delfino S. "Characterization of Fe–Zn–R (R = rare earth metal) crystalline alloys as electrocatalysts for hydrogen evolution". International Journal of Hydrogen Energy. 2008, 33:2660.

[9] Rosalbino F, Macciò D, Saccone A, Angelini E. "Delfino S. Fe–Mo–R (R = rare earth metal) crystalline alloys as a cathode material for hydrogen evolution reaction in alkaline solution". International Journal of Hydrogen Energy. 2011, 36:1965.

[10] Tran M, Dubot P, Sutter EMM. "Activation of water reduction in the presence of REM salts in aqueous solution". International Journal of Hydrogen Energy. 2008, 33:937.

[11] Zhang K, Li J, Liu W, Liu J, Yan C. "Electrocatalytic activity and electrochemical stability of Ni–S/CeO_2 composite electrode for hydrogen evolution in alkaline water electrolysis". International Journal of Hydrogen Energy. 2016, 41:22643.

[12] Zheng Z, Li N, Wang C-Q, Li D-Y, Meng F-Y, Zhu Y-M, et al. "Electrochemical synthesis of Ni–S/CeO_2

composite electrodes for hydrogen evolution reaction". Journal of Power Sources. 2013, 230:10.

[13] Dalla Corte DA, Torres C, Correa PdS, Rieder ES, Malfatti CdF. "The hydrogen evolution reaction on nickel-polyaniline composite electrodes". International Journal of Hydrogen Energy. 2012, 37:3025.

[14] Domínguez-Crespo MA, Torres-Huerta AM, Brachetti-Sibaja B, Flores-Vela A. "Electrochemical performance of Ni–RE (RE = rare earth) as electrode material for hydrogen evolution reaction in alkaline medium". International Journal of Hydrogen Energy. 2011, 36:135.

[15] Madram AR, Pourfarzad H, Zare HR. "Study of the corrosion behavior of electrodeposited Ni–P and Ni–P–C nanocomposite coatings in 1 M NaOH". Electrochimica Acta. 2012, 85:263.

[16] Karimi Shervedani R, Reza Madram A. Electrocatalytic activities of nanocomposite Ni81P16C3 electrode for hydrogen evolution reaction in alkaline solution by electrochemical impedance spectroscopy". International Journal of Hydrogen Energy. 2008, 33:2468.

[17] Shervedani RK, Lasia A. "Studies of the Hydrogen Evolution Reaction on Ni-P Electrodes". Journal of The Electrochemical Society. 1997, 144:511.

[18] Chen Z, Shao G, Ma Z, Song J, Wang G, Huang W. "Preparation of Ni–CeO_2 composite coatings with high catalytic activity for hydrogen evolution reaction". Materials Letters. 2015, 160:34.

[19] Santos DMF, Amaral L, Šljukić B, Macciò D, Saccone A, Sequeira CAC. "Electrocatalytic Activity of Nickel-Cerium Alloys for Hydrogen Evolution in Alkaline Water Electrolysis". Journal of The Electrochemical Society. 2014, 161:F386.

[20] Herraiz-Cardona I, Ortega E, Antón JG, Pérez-Herranz V. "Assessment of the roughness factor effect and the intrinsic catalytic activity for hydrogen evolution reaction on Ni-based electrodeposits". International Journal of Hydrogen Energy. 2011, 36:9428.

[21] Shervedani RK, Madram AR. "Kinetics of hydrogen evolution reaction on nanocrystalline electrodeposited Ni62Fe35C3 cathode in alkaline solution by electrochemical impedance spectroscopy". Electrochimica Acta. 2007, 53:426.

[22] Santos DMF, Sequeira CAC, Figueiredo JL. "Hydrogen production by alkaline water electrolysis". Química Nova. 2013, 36:1176.

[23] Zeng K, Zhang D. "Recent progress in alkaline water electrolysis for hydrogen production and applications". Progress in Energy and Combustion Science. 2010, 36:307.

[24] Navarro-Flores E, Chong Z, Omanovic S. "Characterization of Ni, NiMo, NiW and NiFe electroactive coatings as electrocatalysts for hydrogen evolution in an acidic medium". Journal of Molecular Catalysis A: Chemical. 2005, 226:179.